Magn Reson Mater Phy (2006) 19: 180–186
DOI 10.1007/s10334-006-0039-x

RESEARCH ARTICLE

High proton relaxivity for gadolinium oxide nanoparticles

Maria Engström
Anna Klasson
Henrik Pedersen
Cecilia Vahlberg
Per-Olov Käll
Kajsa Uvdal

Received: 16 February 2006
Revised: 18 May 2006
Accepted: 20 June 2006
Published online: 15 August 2006

M. Engström (✉) · A. Klasson
CMIV, Linköping University,
581 85 Linköping, Sweden
E-mail: maria.engstrom@cmiv.liu.se
Tel.: +46-13-228901

M. Engström · A. Klasson
Department of Radiology,
Linköping University,
581 85 Linköping, Sweden

H. Pedersen · P-O. Käll
Department of Physics, Chemistry and
Biology, Linköping University,
581 83 Linköping, Sweden

C. Vahlberg · K. Uvdal
Department of Physics and Measurement
Technology/Applied Physics,
Linköping University, 581 83 Linköping,
Sweden

Abstract *Objective*: Nanosized materials of gadolinium oxide can provide high-contrast enhancement in magnetic resonance imaging (MRI). The objective of the present study was to investigate proton relaxation enhancement by ultrasmall (5 to 10 nm) Gd_2O_3 nanocrystals.
Materials and methods: Gd_2O_3 nanocrystals were synthesized by a colloidal method and capped with diethylene glycol (DEG). The oxidation state of Gd_2O_3 was confirmed by X-ray photoelectron spectroscopy. Proton relaxation times were measured with a 1.5-T MRI scanner. The measurements were performed in aqueous solutions and cell culture medium (RPMI).
Results: Results showed a considerable relaxivity increase for the Gd_2O_3–DEG particles compared to Gd-DTPA. Both T_1 and T_2 relaxivities in the presence of Gd_2O_3–DEG particles were approximately twice the corresponding values for Gd–DTPA in aqueous solution and even larger in RPMI. Higher signal intensity at low concentrations was predicted for the nanoparticle solutions, using experimental data to simulate a T_1-weighted spin echo sequence.
Conclusion: The study indicates the possibility of obtaining at least doubled relaxivity compared to Gd–DTPA using Gd_2O_3–DEG nanocrystals as contrast agent. The high T_1 relaxation rate at low concentrations of Gd_2O_3 nanoparticles is very promising for future studies of contrast agents based on gadolinium-containing nanocrystals.

Keywords Gd_2O_3 · Nanoparticle · Contrast agent · Relaxivity · MRI

Introduction

Magnetic resonance imaging, which is one of the most important tools for medical image diagnostics, is characterized by its high spatial resolution and unique ability to distinguish soft tissue. There is, however, an increased demand for new and more selective contrast agents for better delineation of different tissues to obtain more precise and earlier diagnosis of diseases. Molecular processes can be studied by positron emission tomography (PET) using radioactive tracers. Recently similar possibilities have been launched for MRI through novel types of contrast agents, such as superparamagnetic nanoparticles. New methods for magnetic tracing provide enhanced possibilities for in vivo cell and molecular MRI [1–4]. One of the aims of the research within molecular MRI is to achieve high sensitivity combined with high spatial

resolution. In addition, suitable combinations of imaging and therapeutic agents will make studies on drug delivery and early evaluation of therapy possible.

Until now, MRI contrast agents have comprised paramagnetic chelates or superparamagnetic iron oxide nanoparticles. Chelates of Gd^{3+} are the most commonly used contrast agents in clinical MRI. However, the relative weak signal intensity enhancement of such agents makes them less suitable for molecular imaging. Preparation of biocompatible nanoparticles with unique magnetic properties is highly interesting for the development of the new generation MRI contrast media [4]. Nanoparticles are promising candidates for molecular imaging compared to chelates because they convey the possibility of high relaxivity per molecular binding site. Using nanoparticles with a ligand that is specific for a certain tissue will enhance the local contrast due to the high relaxivity of each particle. Exploring and optimizing the contrast properties of superparamagnetic nanoparticles are important steps in the search for novel effective agents that allow contrast enhancement at low concentrations.

In this study, the ability to perform proton relaxation by small gadolinium oxide nanoparticles is evaluated. Nanocrystals of gadolinium oxide (Gd_2O_3) coated with diethylene glycol (DEG) were synthesized, characterized by X-ray photoelectron spectroscopy (XPS), and investigated by MRI relaxometry. Proton relaxivity of Gd_2O_3 particles was compared with gadolinium chelates, which are used as contrast agents today. For comparison, it can be mentioned that proton relaxivity for Gd_2O_3 particles of size 20 to 40 nm have been investigated by McDonald and Watkin [5,6]. In the present study ultrasmall Gd_2O_3 particles (5 to 10 nm) were used to study the proton relaxivity [7].

Materials and methods

Synthesis of Gd_2O_3 nanocrystals

Gadolinium oxide nanocrystals were synthesized by the polyol method.

Gd_2O_3–diethylene glycol (1)

$Gd(NO_3)_3{\cdot}6H_2O$ (2 mmol), solid NaOH (2.5 mmol), and a few drops of deionised water were dissolved in 15 ml DEG [$(HOCH_2CH_2)_2O$]. The mixture was heated to 140°C, and when the reactants had dissolved completely, the temperature was raised to 180°C and held constant for 4 h, yielding a dark yellow colloid. The colloid was diluted with deionised water to adjust the gadolinium-oxide concentration to a predetermined value, e.g., 2.5 mM.

Gd_2O_3- diethylene glycol (2)

$GdCl_3{\cdot}6H_2O$ (2 mmol) was dissolved in 10 ml DEG by heating the mixture to 140°C. Solid NaOH (2.5 mmol) was dissolved in 5 ml DEG and subsequently added to the Gd-containing solution. The temperature of the mixture was raised to 180°C and held constant for 4 h under reflux and magnetic stirring, yielding a dark yellow colloid. More details of the synthesis can be found in [7–10].

Studies have shown that Gd_2O_3 nanocrystals prepared by the DEG method are largely crystalline with sizes in a range of 5 to 10 nm [7,9,10].

Sample preparation

X-ray Photoelectron Spectroscopy

The chemical composition of the synthesized nanoparticles were investigated by X-ray photoelectron spectroscopy (XPS). The XPS samples were prepared as follows: the silicon (SiO_x) substrates were first cleaned using a 6:1:1 mixture of MilliQ water: HCl (37%): H_2O_2 (28%) for 5–10 min at 80°C followed by a 5:1:1 mixture of MilliQ water: NH_3 (25%): H_2O_2 (28%) for 5–10 min at 80°C. After each washing step the silicon surfaces were carefully rinsed with MilliQ water. Gd_2O_3–DEG was mixed with basic MilliQ water and spin-coated onto freshly cleaned silicon (SiO_x) substrates at a rate of 2000 rpm and then immediately placed in the XPS instrument.

Relaxivity measurements

Samples of Gd_2O_3–DEG, and Gd–diethylenetriamine-pentaacetate (Gd-DTPA, Magnevist)® were prepared in 10 mm NMR test tubes with H_2O, 1 M hydroxylamine buffer ($NH_2(OH)/NH_3(OH)^+$) and in RPMI 1640 cell culture medium with 10% fetal calf serum (FCS) (GIBCO, Invitrogen, Carlsbad, CA, USA) in Gd concentrations of 0.1 to 1.6 mM. During measurement the test tubes were immersed in a bowl with saline at 21 to 23°C, the temperature of the scanner room. pH was measured by a Metrohm 744-pH meter and also checked by pH-indicator strips (Merck).

The Gd contents in nanoparticle stem solutions were determined by inductively coupled plasma sector field mass spectrometry (ICP-SFMS) at Analytica AB (Luleå, Sweden). Before measuring the concentrations the samples were diluted 1:100,000 with 1% HNO_3.

X-ray Photoelectron Spectroscopy

The XPS spectra for Gd_2O_3–DEG(1) were recorded on a VG instrument using unmonochromatized Al Kα photons (1,486.6 eV) and a CLAM2 analyzer. The power of the X-ray gun was 300 W. The spectra were based upon photoelectrons with a takeoff angle of 30° relative to the normal of the substrate surface. The pressure in the analysis chamber was $\sim 3 \times 10^{-10}$ mbar and the temperature was $\sim$ 297 K during the measurements.

VGX900 data analysis software was used to analyze the peak position.

Relaxivity measurements

The T_1 and T_2 relaxation times were measured with a 1.5-T Philips Achieva whole-body scanner using the head coil. A 2D mixed multiecho SE interleaved with multiecho IR sequence was used for the measurements [11]. Imaging time parameters were varied to minimize the standard deviations in relaxation time calculations: TE = 30 ms, TR (SE) = 500 ms, TI = 150 ms, and TR (IR) = 1,150 ms (set 1); TE = 50 ms, TR (SE) = 760 ms, TI = 370 ms, and TR (IR) = 2290 ms (set 2). Other MR parameters were: FOV = 23 cm, slice thickness = 7 mm, number of echoes = 4.

Results

X-ray Photoelectron Spectroscopy

XPS was used to study the composition and binding energy of Gd_2O_3–DEG. A wide-scan spectrum of the Gd_2O_3–DEG(1) nanoparticles spin-coated onto a silicon substrate is presented in Fig. 1. The most intense photoelectron binding energy peaks are the ones at 1220 and 1188 eV, corresponding to Gd ($3d_{3/2}$) and Gd ($3d_{5/2}$), respectively. The peak positions are consistent with the energy level for Gd in Gd_2O_3 [12], thus verifying the oxidation state of the sample. The O (1s) peak is found at 532 eV. This peak is a sum of three different oxygen-containing compounds, i.e., Gd_2O_3, the capping DEG molecule and the silicon (SiO_x) substrate. The two Si (2*s*) and Si (2*p*) binding energy peaks at 151 and 99 eV originate from the substrate. The film of spin-coated Gd_2O_3–DEG was thin in order to minimize charging effects during the XPS measurements. The prominent peak found at 978 eV originates from the O (KLL) Auger line. A more detailed analysis of the coordination geometry of the capping molecules onto the rare earth nanoparticles is published elsewhere [7, 13].

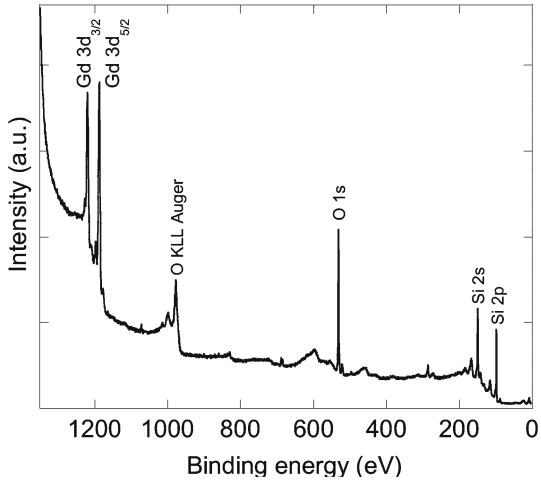

Fig. 1 Wide-scan XPS spectrum of Gd_2O_3–DEG(1) nanoparticles spin-coated onto a silicon substrate

Relaxivity measurements

In this study, Gd_2O_3–DEG nanoparticles induced higher proton relaxivities compared to Gd–DTPA chelate (Magnevist®). The values of the relaxivity constants, r_1 and r_2, for Gd_2O_3–DEG and Gd–DTPA in three different media [H_2O, H_2O + buffer, and cell culture medium (RPMI)] are given in Table 1. It is clearly shown that the relaxivities due to the nanoparticles were twice that of the chelate for Gd_2O_3–DEG(1) in H_2O solution and almost twice that for Gd_2O_3–DEG(2) in buffer where in the latter r_1(particle)/r_1(chelate) = 1.8, r_2(particle)/ r_2(chelate) = 1.9. In RPMI the relaxivity differences between particles and chelate were even more pronounced: r_1(particle)/r_1(chelate) = 2.6 and 2.7, r_2(particle)/r_2(chelate) = 3.8 and 3.5 for Gd_2O_3–DEG(1) and Gd_2O_3–DEG(2), respectively. Both r_1 and r_2 for the Gd_2O_3 particles were substantially increased when measured in RPMI compared to H_2O or buffer. Relative increases, r_i(RPMI)/r_i(H_2O/buffer), were 1.4 for both Gd_2O_3–DEG samples and 2.2 [Gd_2O_3–DEG(1)] and 1.9 [Gd_2O_3–DEG(2)] for r_1 and r_2, respectively. This should be compared with the less increased relaxivity of Gd–DTPA: r_i(RPMI)/r_i(H_2O) = 1.1 and 1.2 for r_1 and r_2, respectively.

Table 1 Relaxivity constants (r_1, r_2) in s^{-1} mM^{-1}, standard deviation (SD), and P-values for Gd–DTPA and Gd_2O_3–DEG in H_2O, buffer, and cell culture medium (RPMI) measured at 1.5 T, 21–23°C

	r_1	SD	P	r_2	SD	P	pH
H_2O							
Gd–DTPA	4.7	±0.1	<0.0001	5.3	±0.2	<0.0001	5.4
Gd_2O_3–DEG(1)	9.2	±0.3	<0.0001	11.3	±0.4	<0.0001	6.3–7.2
Buffer							
Gd–DTPA	5.6	±0.3	<0.0001	6.2	±0.3	<0.0001	7.2
Gd_2O_3–DEG(2)	9.8	±0.5	<0.0001	11.9	±0.7	<0.0001	7.4
RPMI							
Gd–DTPA	5.1	±0.1	<0.0001	6.4	±0.1	<0.0001	7.3
Gd_2O_3–DEG(1)	13.2	±0.7	<0.0001	24.6	±2.3	0.0003	7.3
Gd_2O_3–DEG(2)	13.9	±0.8	<0.0001	22.3	±1.9	0.0017	7.3

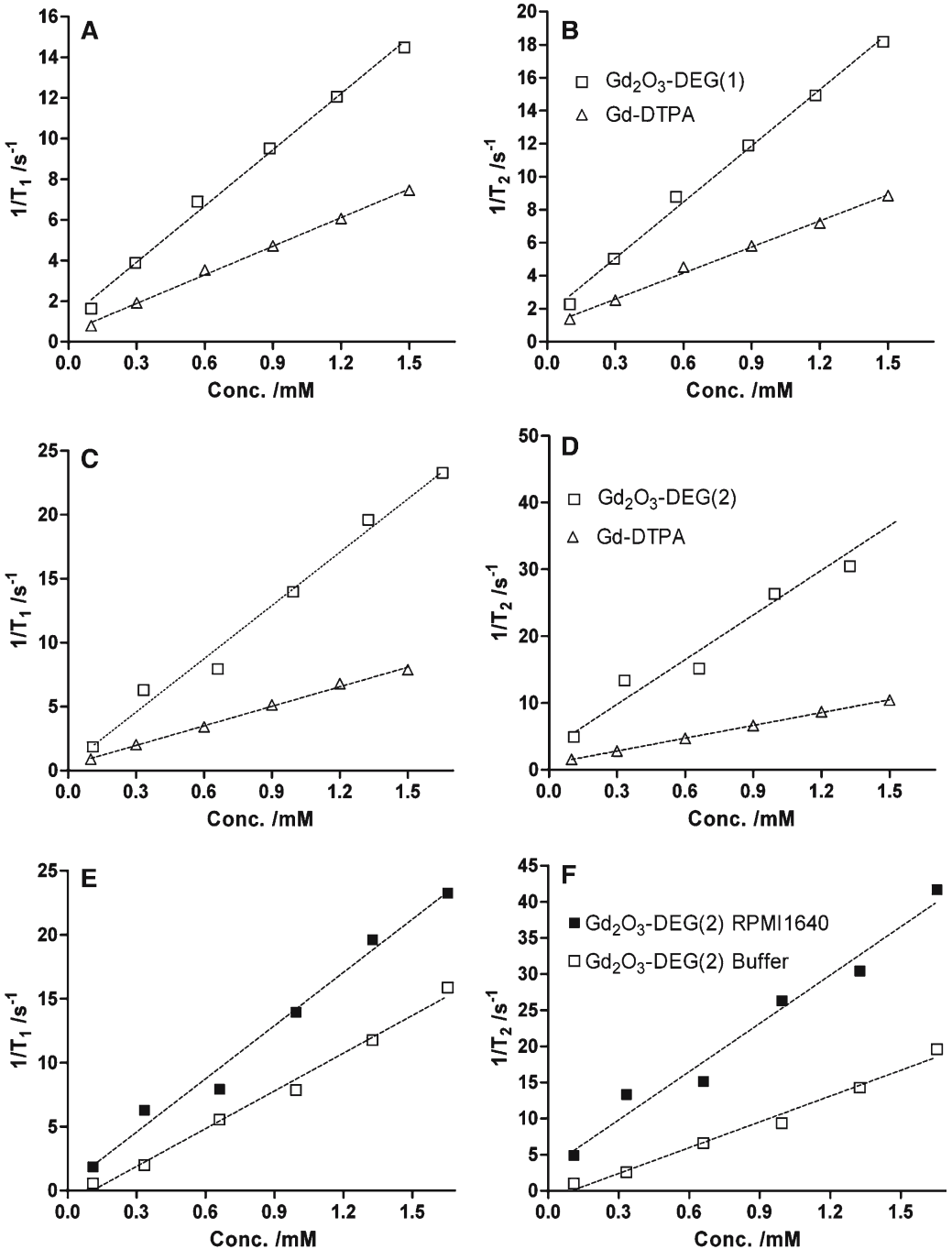

Fig. 2 Experimentally measured relaxation rates and corresponding calculated regression slopes. The concentration is given in mM Gd. **a, b** $1/T_1$ and $1/T_2$ for Gd_2O_3–DEG(1) and Gd–DTPA in H_2O. The regression shows a goodness of fit of $r^2 > 0.99$ for both $1/T_1$ and $1/T_2$ for both samples. **c, d** $1/T_1$ and $1/T_2$ for Gd_2O_3–DEG(2) and Gd–DTPA in cell culture medium (RPMI). The regression shows a goodness of fit of $r^2 > 0.98$ ($1/T_1$), $r^2 > 0.97$ ($1/T_2$) for Gd_2O_3–DEG(2), and $r^2 > 0.99$ ($1/T_1$, $1/T_2$) for Gd–DTPA. **e, f** $1/T_1$ and **b** $1/T_2$, for Gd_2O_3–DEG(2) in cell culture medium (RPMI) and buffer. The regression shows a goodness of fit of $r^2 > 0.98$ ($1/T_1$), $r^2 > 0.97$ ($1/T_2$) in RPMI and $r^2 > 0.99$ ($1/T_1$) and $r^2 > 0.98$ ($1/T_2$) in buffer

The relaxation rates ($1/T_1$) and ($1/T_2$) as a function of Gd_2O_3–DEG and Gd–DTPA concentration in H_2O, buffer, and cell culture medium are shown in Fig. 2. The plots of $1/T_i$ vs. Gd concentration show a linear relationship according to:

$$\frac{1}{T_i(observed)} = \frac{1}{T_i(0)} + r_i \cdot C, \quad i = 1, 2, \tag{1}$$

where T_i(observed) is the relaxation time in the presence of the contrast agent, $T_i(0)$ is the diamagnetic contribution to the relaxation time, r_i is the relaxivity constant, i.e., the slope of the line, and C is the Gd concentration. The $1/T_i$ plots for the H_2O samples showed an almost perfect linear relation with a goodness of fit $r^2 > 0.99$ for both samples (Fig. 2a,b). Small deviations from the fit were, however, observed for samples with nanoparticles in RPMI (Fig. 2c,d) [$r^2 > 0.98$ ($1/T_1$), $r^2 > 0.97$ ($1/T_2$)]. The correlation was still high, $r^2 > 0.99$, for Gd–DTPA in RPMI. The relaxation rates in the presence of gadolinium oxide nanoparticles were highly dependent on the solvent (Fig. 2e,f). Both $1/T_1$ and $1/T_2$ were significantly higher in RPMI and buffer compared to H_2O, whereas the relaxation for Gd–DTPA was essentially indifferent to the type of media used in this study (data not shown). These results were also reflected in the relaxivity constants, r_1 and r_2, as shown in Table 1.

Proton relaxation rates in the presence of Gd_2O_3–DEG were found to be pH sensitive as both $1/T_1$ and $1/T_2$ decreased at higher pH (Fig. 3). The concentration of the solution was found to influence the pH of the H_2O samples, increasing from pH = 6.3 at 0.3 mM to 7.2 at 1.5 mM, possibly due to traces of hydroxide from the synthesis. The measurements in H_2O are therefore likely to be slightly affected by the pH variation (Fig. 2a,b). However, pH did not vary with concentration for the Gd_2O_3–DEG and Gd–DTPA samples in buffer (pH = 7.4 and 7.2, respectively) or in RPMI (pH = 7.3).

To estimate the signal intensity for a T_1-weighted (T1W) sequence, the measured relaxation times were inserted into the theoretical expression for a spin echo sequence:

$$S(\mathrm{TR}, \mathrm{TE}) = \rho e^{-\mathrm{TE}/T_2}(1 - e^{-\mathrm{TR}/T_1}). \quad (2)$$

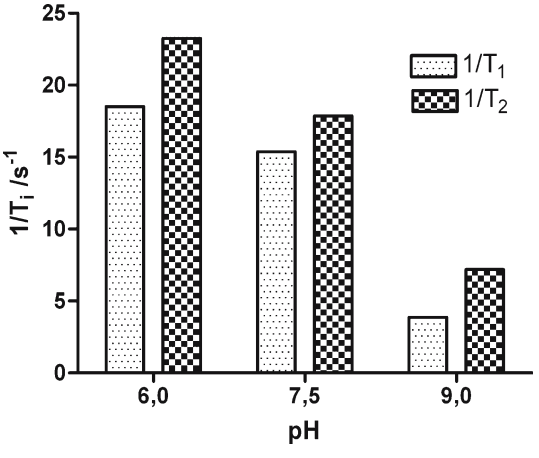

Fig. 3 pH dependence of relaxation rates ($1/T_i$) in Gd_2O_3–DEG(1) H_2O samples

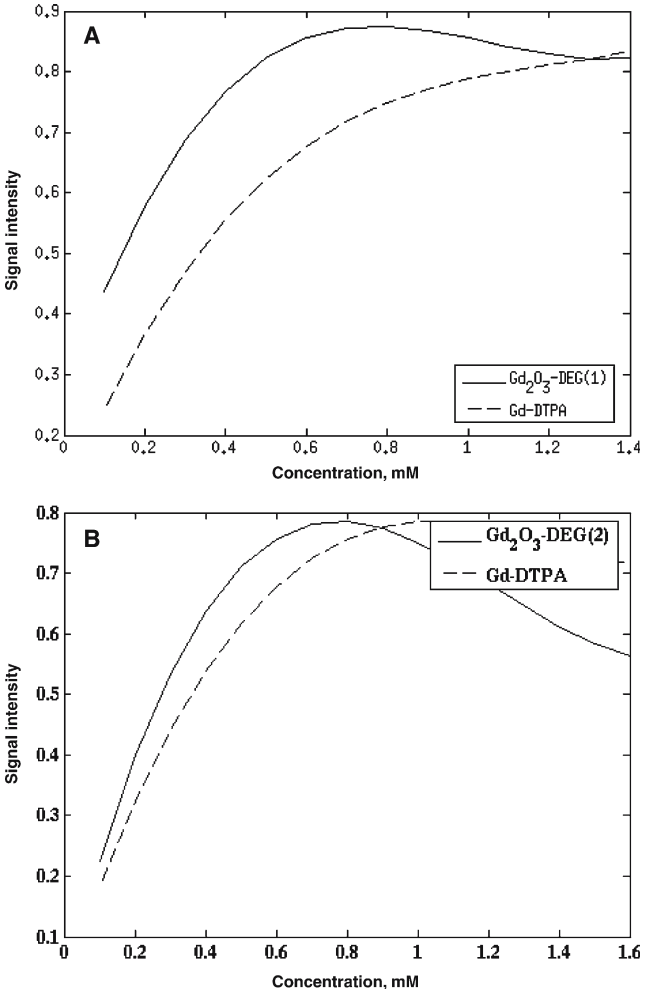

Fig. 4 Simulated signal intensity for Gd_2O_3–DEG and Gd–DTPA. Experimental $1/T_1$ and $1/T_2$ values were inserted in Eq. 2 ($\rho = 1$, TR = 350 ms, TE = 10 ms) and *curve* fitted with third-degree polynomials: **a** H_2O, **b** cell culture medium (RPMI). The concentration is given in mM Gd

Figure 4 shows the simulated intensity curves for Gd_2O_3–DEG samples compared with Gd–DTPA using the following parameters: $\rho = 1$, TE = 10 ms, TR = 350,ms and curve fitting with third-degree polynomials. The signal intensity shows a behavior that is expected for paramagnetic relaxation agents [14]. According to Eq. 2, there is a competing effect of T_1 and T_2 on the signal intensity. That is to say, short T_1 increases the signal whereas short T_2 leads to a signal decrease, and a signal peak occurs at intermediate concentrations. The simulated signal had higher signal intensity at lower concentrations for Gd_2O_3–DEG samples compared with Gd–DTPA. The augmented signal at lower concentrations ($\lesssim 0.7$ mM) of nanoparticle solutions were pronounced for measure-

ments in H_2O (Fig. 4a) and RPMI (Fig. 4b). The steep signal increase at low concentrations can be explained by the high T_1 relaxivity. At higher concentrations ($\gtrsim 1.0$ mM) the strong T_2 effect attenuated the signal in nanoparticle-containing samples to become lower than in Gd–DTPA ones. The pronounced T_2 shortening effect for Gd_2O_3 nanoparticles in cell culture medium (Table 1) explains the fast signal decay in Fig. 4b. For the applied parameters in a simulated T1W sequence the Gd_2O_3–DEG samples reached the signal peak at lower concentrations ($\lesssim 0.7$ mM) compared with the Gd–DTPA signal that peaked outside the employed concentration range.

Discussion

In the present study proton T_1 and T_2 relaxation enhancement by gadolinium oxide nanocrystals was obtained. It is, to our knowledge, the first time relaxation behavior for such ultrasmall (5 to 10 nm) Gd_2O_3 particles are reported. Our results showed a considerable increase in relaxivity in the presence of Gd_2O_3–DEG nanoparticles compared with Gd–DTPA. Another interesting feature was the marked T_1-reducing effect and simulated signal increase at low concentrations ($\lesssim 0.7$ mM). The concentration range below 0.6 mM in plasma is most relevant for clinical use. At the recommended dose of Magnevist, 0.1 mmol/kg, the detected plasma concentration of Gd is 0.6 mM at 3 min after injection and 0.24 mM after 60 min.[1]

There is an inverse relationship between viscosity and T_1 and T_2 [15,16]. It has been shown that Gd–DTPA relaxivity depends on the macromolecular content of the solvent [17]. However, the marked increase in relaxation rates for the Gd_2O_3 nanoparticles in RPMI can probably not be attributed only to increased viscosity and macromolecular content. In the study by Stanisz et al. [17], r_1 increases from 4.5 $s^{-1}\,mM^{-1}$ for Gd–DTPA in pure saline to 5.2 $s^{-1}\,mM^{-1}$ in 10% skim milk solution. These results correspond well with the values for Gd–DTPA in H_2O and RPMI with 10% FCS in the present study (Table 1). However, the increase of r_1 and r_2 for Gd_2O_3–DEG is more prominent than for Gd–DTPA when going from an aqueous solution to RPMI. Studies have shown that macromolecular binding increases rotational correlation time, resulting in an increased relaxivity [18]. We are now investigating whether binding of, e.g., peptides and proteins from the cell culture medium to the nanoparticles is responsible for the increased relaxivity observed in the present study.

The pH dependency was investigated in this study since proton relaxivity of Gd chelates can be sensitive to pH. It has been shown that prototropic exchange is enhanced at higher pH and in buffered solutions, leading to increased relaxivity [19,20]. Gd chelates can also be designed to give essentially constant r_1 in acidic solutions with a marked change in the relaxivity curve at neutral pH toward lower values in basic solutions [21,22]. In those cases, it has been suggested, displacement of coordinated water molecules by formation of complexes with ions present in the aqueous solution is responsible for the r_1 decrease at high pH. The stability of nanocrystalline Gd_2O_3 is, of course, strongly dependent on pH. Even at neutral pH the long-term stability of the particles is limited, implying that a considerable fraction of the material will be present as Gd^{3+} ions. The issue will be dealt with in detail in a forthcoming article by us.

Before considering Gd-containing nanoparticles for clinical use, the issue of particle stability and toxicity obviously must be clarified. Free Gd^{3+} ions are regarded as toxic. This is a main reason why Gd-based contrast agents must be chelated by a stable ligand, e.g., DTPA or incorporated into scaffolds such as liposomes, dendrimers, or other types of polymeric structures [23]. Toxicity for Gd-containing complexes is increased if transmetallation with, e.g., Zn^{2+} and Ca^{2+} occurs, leading to Gd^{3+} release [24]. Another consideration regarding medical application of nanocrystals is the issue of particle agglomeration. Noncoated nanoparticles tend to aggregate due to attractive electrostatic forces [25]. Molecular coating of the nanoparticles brings about both increased colloidal stabilty, i.e., less agglomeration, and a suitable surface for biofunctionalization [26]. Lebbou et al. found that Eu^{3+} doped Gd_2O_3 solutions are stable for months prepared by the polyol route from gadolinium chloride [27]. However, submicrometric agglomerates are formed when starting from rare earth nitrates.

In conclusion, in this study it was shown that when using Gd_2O_3–DEG nanocrystals as contrast agent at least doubled relaxivity can be obtained compared with Gd–DTPA. The high T_1 relaxation rate at low Gd concentrations ($\lesssim 0.7$ mM) in Gd_2O_3–DEG nanoparticles solutions is promising for contrast enhancement at low doses.

Acknowledgements The Center for Medical Image Science and Visualization (CMIV) at Linköping University, Sweden, is acknowledged for its financial support. This project was partly supported by grants from Carl Tryggers Foundation and local funds at Linköping University Hospital.

[1] www.fass.se, the official Swedish pharmacological information portal.

References

1. Jaffer FA, Weissleder R (2005) Molecular imaging in the clinical arena. J Am Med Assoc 293:855–862
2. Gillies RJ (2002) In vivo molecular imaging. J Cell Biochem 39:231–238
3. Dijkhuizen RM, Nicolay K (2003) Magnetic resonance imaging in experimental brain model of brain disorders. J Cerebr Blood Flow Metabol 23:1383–1402
4. Wickline SA, Lanza GM (2002) Molecular imaging, targeted therapeutics, and nanoscience. J Cell Biochem S39:90–97
5. McDonald MA, Watkin KL (2004) Investigation into the structure and magnetic properties of dextran small particulate gadolinium oxide nanoparticles. In: 12th scientific meeting and exhibition, International Society for Magnetic Resonance in Medicine (ISMRM), Kyoto, Japan, p 1718
6. McDonald MA, Watkin KL (2003) Small particulate gadolinium oxide and gadolinium oxide albumin microspheres as multimodal contrast and therapeutic agents. Invest Radiol 38:305–310
7. Söderlind F, Pedersen H, Petoral RM Jr, Käll P-O, Uvdal K (2005) Synthesis and characterisation of Gd_2O_3 nanocrystals functionalised by organic acids. J Colloid Interface Sci 288:140–148
8. Feldmann C (2003) Polyol-mediated synthesis of nanoscale functional materials. Adv Funct Mater 13:101–107
9. Bazzi R, Flores-Gonzalez MA, Louis C, Lebbou K, Durjardin C, Brenier A, Zhang W, Tillement O, Bernstein E, Perriat P (2003) Synthesis and luminescent properties of sub-5-nm lanthanide oxides nanoparticles. J Luminescence 102:445–450
10. Bazzi R, Flores C, Louis C, Lebbou K, Zhang W, Durjardin C, Roux S, Mercier B, Ledoux G, Bernstein E, Perriat P, Tillement O (2004) Synthesis and properties of europium-based phosphors on the nanometer scale: Eu_2O_3, Gd_2O_3:Eu, and Y_2O_3:Eu. J Colloid Interface Sci 273:191–197
11. In den Kleef JJE, Cuppen JJM (1987) RLSQ: T1, T2 and RHO calculations, combining ratios and least squares. Magn Res Med 5:513–524
12. Raiser D, Deville JP (1991) Study of XPS photoemission of some gadolinium compounds. J Electron Spectrosc 57:91–97
13. Pedersen H, Söderlind F, Petoral RM, Uvdal K, Käll PO, Ojamäe L (2005) Surface interactions betweenY(2)O(3) nanocrystals and organic molecules – an experimental and quantum-chemical study. Surf Sci 592:124–140
14. Hendrick RE, Haacke EM (1993) Basic physics of MR contrast agents and maximization of image contrast. J Magn Res Imag 3:137–148
15. Bloembergen N, Purcell EM, Pound RV (1948) Relaxation effects in nuclear magnetic resonance absorption. Phys Rev 73:679–712
16. Nelson TR, Tung SM (1987) Temperature dependence of proton relaxation times in vitro. Magn Reson Imag 5:189–199
17. Stanisz GJ, Henkelman RM (2000) Gd–DTPA relaxivity depends on macromolecular content. Magn Red Med 44:665–667
18. Lauffer RB (1987) Paramagnetic metal complexes as water proton relaxation agents for NMR imaging: theory and design. Chem Rev 87:901–927
19. Aime S, Barge A, Botta M, Parker D, De Sousa AS (1997) Prototropic vs whole water exchange contribution to the solvent relaxation enhancement in the aqueous solution of a cationic Gd^{3+} macrocyclic complex. J Am Chem Soc 119:4767–4768
20. Aime S, Botta M, Fasano M, Paoletti S, Terreno E (1997) Relaxometric determination of the exchange rate of the coordinated water protons in a Neutral Gd^{III} chelate. Chem Eur J 3:1499–1504
21. Botta M, Aime S, Barge A, Bobba G, Dickins RS, Parker D, Terreno E (2003) Ternary complexes between cationic Gd^{III} chelates and anionic metabolites an aqueous solution: an NMR relaxometric study. Chem Eur J 9:2102–2109
22. Lowe MP, Parker D, Reany O, Aime S, Botta M, Castellano G, Gianolio E, Pagliarin R (2001) pH-dependent modulation of relaxivity and luminescence in macrocyclic gadolinium and europium complexes based on reversible intramolecular sulfonamide ligation. J Am Chem Soc 123:7601–7609
23. Reynolds CH, Annan N, Beshah K, Huber JH, Shaber SH, Lenkinski RE, Wortman JA (2000) Gadolinium-loaded nanoparticles: new contrast agents for magnetic resonance imaging. J Am Chem Soc 122:8940–8945
24. Cacheris WP, Quay SC, Rocklage SM (1990) The relationship between thermodynamics and the toxicity of gadolinium complexes. Magn Res Imag 8:467–481
25. Bruemmel Y, Chan CP, Renneberg R, Thuenemann A, Seydack M (2004) On the influence of different surfaces in nano- and submicrometer particle based fluorescence immunoassays. Langmuir 20:9371–9379
26. Nichkova M, Dosev D, Gee SJ, Hammock BD, Kennedy IM (2005) Microarray immunoassay for phenoxybenzoic acid using polymer encapsulated Eu:Gd_2O_3 nanoparticles as fluorescent labels. Anal Chem 77:6864–6873
27. Lebbou K, Perriat P, Tillement O (2005) Recent progress on elaboration of undoped and doped Y_2O_3, Gd_2O_3 rare earth nano-oxide. J Nanosci Nanotechnol 5:1448–1454